



This is a repository copy of *On the Analogy Between Vehicle and Vehicle-Like Cavities With Reverberation Chambers*.

White Rose Research Online URL for this paper:  
<http://eprints.whiterose.ac.uk/90834/>

Version: Accepted Version

---

**Article:**

Herbert, S., Loh, T-H., Wassell, I. et al. (1 more author) (2014) On the Analogy Between Vehicle and Vehicle-Like Cavities With Reverberation Chambers. *IEEE Transactions on Antennas and Propagation*, 62 (12). 6236 - 6245. ISSN 0018-926X

<https://doi.org/10.1109/TAP.2014.2363681>

---

**Reuse**

Unless indicated otherwise, fulltext items are protected by copyright with all rights reserved. The copyright exception in section 29 of the Copyright, Designs and Patents Act 1988 allows the making of a single copy solely for the purpose of non-commercial research or private study within the limits of fair dealing. The publisher or other rights-holder may allow further reproduction and re-use of this version - refer to the White Rose Research Online record for this item. Where records identify the publisher as the copyright holder, users can verify any specific terms of use on the publisher's website.

**Takedown**

If you consider content in White Rose Research Online to be in breach of UK law, please notify us by emailing [eprints@whiterose.ac.uk](mailto:eprints@whiterose.ac.uk) including the URL of the record and the reason for the withdrawal request.



[eprints@whiterose.ac.uk](mailto:eprints@whiterose.ac.uk)  
<https://eprints.whiterose.ac.uk/>

# On the Analogy Between Vehicle and Vehicle-like Cavities with Reverberation Chambers

Steven Herbert, *Student Member, IEEE*, Tian-Hong Loh, *Member, IEEE*, Ian Wassell, and Jonathan Rigelsford, *Senior Member, IEEE*

**Abstract**—Deploying wireless systems in vehicles is an area of current interest. Often, it is implicitly assumed that the electromagnetic environment in vehicle cavities is analogous to that in reverberation chambers, it is therefore important to assess to what extent this analogy is valid. Specifically, the cavity time constant, electromagnetic isolation and electric field uniformity are investigated for typical vehicle and vehicle-like cavities.

It is found that the time constant is a global property of the cavity (i.e., it is the same for all links). This is important, as it means that the root mean square delay spread for any link is also a property of the cavity, and thus so is the coherence bandwidth. These properties could be exploited by wireless systems deployed in vehicles. It is also found that the field distribution is not homogeneous (and is therefore not uniform), but can be isotropic. For situations where the field distribution is isotropic, the spatial coherence is well defined, and therefore Multiple-Input-Multiple-Output antenna arrays can be used to improve performance of wireless systems. For situations where the field distribution is not isotropic, the angular spread is not uniform, and therefore beam-forming can be used to improve performance of wireless systems.

**Index Terms**—Vehicle cavities, electromagnetic cavities, reverberation chambers, wireless communications.

## I. INTRODUCTION

UNDERSTANDING the propagation of electromagnetic waves in vehicles is an area of current relevance. This is due to the prevalence of wireless communication systems in vehicles, such as ‘infotainment’ systems, vehicle radio, Wi-Fi, Bluetooth and wireless sensor networks (WSNs) [1]. Furthermore, there is interest in using wireless systems to reduce the weight and installation costs of systems which could potentially use wires [2]. A large body of existing published work seeks to apply reverberation chamber-like methods to characterise the electromagnetic propagation and

field distributions in vehicles [3]–[7]. Specifically, the reverberation chamber has five definitive properties, and we investigate to what extent these are valid for vehicle cavities:

- 1) The energy retained in the cavity at time  $t$ , after a unit impulse input of energy at  $t = 0$  is proportional to  $e^{-\frac{t}{\tau}}$ , where  $\tau$  is the cavity time constant.
- 2) The reverberation chamber is an isolated Electromagnetic (EM) environment.
- 3) Within the working volume, the Electric field (E-field) distribution is isotropic.
- 4) Within the working volume, the E-field distribution is homogeneous.
- 5) Within the working volume, the E-field distribution is ergodic, i.e., the same field distribution can be obtained by sampling in frequency, space or time (if a well designed stirrer is deployed to vary the field).

Where the working volume is defined for any given reverberation chamber as a certain number of half-wavelengths from the cavity walls. Together, points 3), 4) and 5) define a *uniform* E-field distribution. With regard to point 5), under normal operating conditions, vehicle cavities do not, in general, have well designed stirrers, therefore the property of ergodicity is limited to the frequency and spatial domains for the purposes of vehicle cavities (although it should be noted that a stirrer has been introduced for some of the experiments presented in this paper). Furthermore, the time variation of the in-vehicle E-field depends on the motion of the cavity occupants, which is not trivial to model, and is not within the scope of this paper. For a characterisation of the time variation and Doppler spread of in-vehicle wireless communication channels, we refer the reader to our previous work [8].

The paper is organised as follows: Details of the experimental methods undertaken are given in Section II; Section III presents the outcomes of the investigation into points 1)-5) (above); Section IV presents a proposed cavity classification method which helps enable reverberation chamber analysis to find parameters such as the Root-Mean Square (RMS) delay spread, angular spread and coherence distance, which are useful for the design and evaluation of in-vehicle communication systems; and finally conclusions are drawn in Section V.

## II. EXPERIMENTAL METHOD

We undertook three measurement campaigns. The first two were undertaken in a vehicle-like cavity located in a

This work is supported by the U.K. Engineering and Physical Sciences Research Council (EPSRC) and National Physical Laboratory (NPL) under an EPSRC-NPL Industrial CASE studentship programme on the subject of Intra-Vehicular Wireless Sensor Networks. The work of T. H. Loh was supported by the 2009 - 2012 Physical Program and 2012 - 2015 Electromagnetic Metrology Program of the National Measurement Office, an Executive Agency of the U.K. Department for Business, Innovation and Skills, under Projects 113860 and EMT13020, respectively.

Steven Herbert is with the Computer Laboratory, University of Cambridge, CB3 0FD, UK, and the National Physical Laboratory, TW11 0LW, UK. Contact: sjh227@cam.ac.uk

Tian Hong Loh is with the National Physical Laboratory, TW11 0LW, UK. Contact: tian.loh@npl.co.uk

Ian Wassell is with the Computer Laboratory, University of Cambridge, CB3 0FD, UK. Contact: ijw24@cam.ac.uk

Jonathan Rigelsford is with the Department of Electronic & Electrical Engineering, University of Sheffield, S1 3JD, UK. Contact: j.m.rigelsford@sheffield.ac.uk

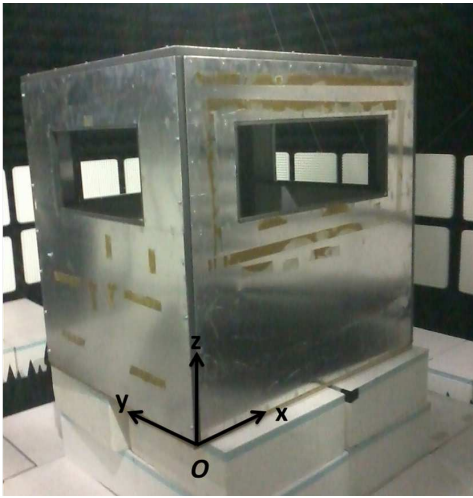


Fig. 1. The SEFERE vehicle-like cavity.

fully anechoic chamber; and the third was undertaken in two actual vehicles. Furthermore, ray tracing and CST Microwave Studio [9] simulations were undertaken for the vehicle-like cavity.

The vehicle-like cavity used is that from the ‘SEFERE’ project [10], [11]. It has been shown that the difference in terms of electromagnetic environment between the vehicle-like cavity and actual vehicles is minimal [12]–[14]. During the measurement process the vehicle-like cavity was located in the UK National Physical Laboratory Small Antenna Radiated Testing (SMART) range, enabling us to isolate the cavity from the effects of external objects and noise sources (which would otherwise not have been possible). The measurement set-up is shown in Figure 1, with origin and axes definitions. Figure 2 shows a plan-view diagram of the cavity, which has dimensions 1260 mm  $\times$  1050 mm  $\times$  1220 mm ( $x \times y \times z$ ). It has four rectangular apertures with corners located at:

- 1) (0, 230, 700) mm, (0, 230, 1000) mm, (0, 820, 700) mm, (0, 820, 1000) mm;
- 2) (1260, 230, 700) mm, (1260, 230, 1000) mm, (1260, 820, 700) mm, (1260, 820, 1000) mm;
- 3) (230, 0, 700) mm, (230, 0, 1000) mm, (1030, 0, 700) mm, (1030, 0, 1000) mm;
- 4) (230, 1050, 700) mm, (230, 1050, 1000) mm, (1030, 1050, 700) mm, (1030, 1050, 1000) mm.

The actual vehicles used were an estate car, shown in Figure 3, and a panel van shown in Figure 4.

#### A. Using mechanical and frequency stirring to investigate the E-field distribution

This measurement took place in the vehicle-like cavity. A Rohde & Schwarz ZVB four-port vector network analyser (VNA) was used, with each port connected, via coaxial cables, to Schwarzbeck 9113 antennas [15]. Port 1 acted as a transmitter and ports 2, 3 and 4, orientated such that they

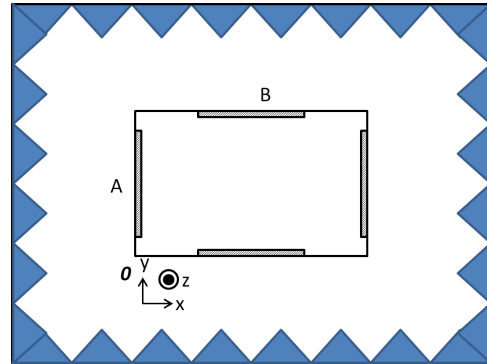


Fig. 2. Plan view of the SEFERE vehicle-like cavity, with locations of external objects ‘A’ and ‘B’.



Fig. 3. The road car, with port 1 antenna in the boot.



Fig. 4. The panel van.

are mutually orthogonally polarised, acted as receivers. The antennas were located and polarised as follows:

- Port 1: (1020, 880, 510) mm,  $x$  and  $z$  polarised;
- Port 2: (300, 490, 440) mm,  $z$  polarised;
- Port 3: (256, 210, 810) mm,  $x$  polarised;
- Port 4: (300, 470, 440) mm,  $y$  polarised,

i.e., the three mutually orthogonal receivers were close to each other, and reasonably far from the transmitter. The direct line between the transmitter and each of the receivers was blocked as explained in the next paragraph ( $x$  polarised refers to the antenna orientation, such that the direction of maximum E-field is parallel to the  $x$  axis and likewise for  $y$  and  $z$ ).

The channels created are referred to by the subscript  $mn$ , where  $m$  is the transmitter polarisation, and  $n$  is the receiver polarisation, e.g.,  $E_{xx}$  would refer to the electric

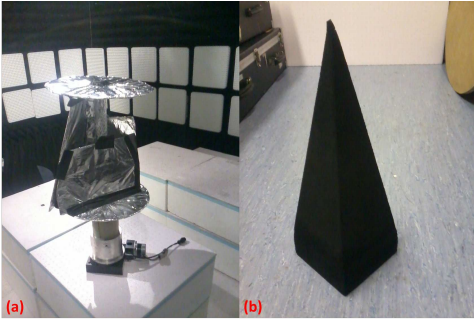


Fig. 5. (a): The stirrer unit; (b) a single unit of RAM.

field measured for the channel with both antennas  $x$  polarised. The VNA was set to sweep from 500 to 3000 MHz, at a resolution of 5 MHz. A stirrer, shown in Figure 5 (a) was deployed within the vehicle-like cavity, obscuring the direct line between the transmitter and each of the three receive antennas. The stirrer operated in stirred mode at 0.0044 revolution/ s, approximately 90 measurements were taken in a full revolution, of which 15 were independent at 3 GHz (i.e., according to the criteria defined in IEC 61000-4-21 [16]). Therefore 15 stirrer positions were used, although these would not have been independent for lower frequency values. The stirrer has height 410 mm and diameter 360 mm, which is smaller than the maximum wavelength used of 600 mm (i.e., at 500 MHz).

For each frequency, the response at the 15 stirrer positions is used to plot the E-field distribution (i.e., by noting that the magnitude of the forward voltage gain is proportional to the E-field). In Section IV, however, we see that this may not be sufficient to obtain an isotropic field (even at arbitrarily high operating frequencies), we therefore introduce some frequency diversity to improve the uniformity of the field. We achieve this by including the frequency responses out to  $\pm 50$  MHz relative to the central frequency. We refer to this as frequency stirring (even though it differs slightly from typical reverberation chamber frequency stirring [17], [18]), and in effect we have included frequency samples spanning multiple coherence bandwidths (approximately 4, according to [19]) to improve the field uniformity, at the cost of some resolution in the frequency domain (i.e., we can only now consider frequency samples spaced by 100 MHz).

We further vary the operating conditions by introducing into the vehicle-like cavity, Radiation Absorbent Material (RAM), one unit of which consists of a square based pyramid with base of side 150 mm and vertical height 390 mm, on top of a cuboid of height 50 mm, which is shown in Figure 5 (b). We investigate four scenarios, where the number of units of RAM are: 0; 4; 8; and 12, and in each case the RAM is positioned randomly on the cavity floor.

We also measured the same RAM configurations, with the stirrer stationary in the cavity, to perform a frequency sweep from which we can find the impulse response. In this case we

use only the data between 1 to 3 GHz, as between 500 MHz to 1 GHz we do not know the efficiency of the antenna. We use a similar method to that in [ [7] Section III] (in fact our method here has been simplified, as we do not need to find an exact discrete representation of the arriving rays) to find the impulse response from the frequency response, specifically:

$$P = \left| \text{IDFT} \left( \frac{\mathbf{S}_{\alpha 1} \odot \mathbf{f}}{\sqrt{\eta_{tx} \eta_{rx}}} \right) \right|^2, \quad (1)$$

where  $P$  is the received power after an impulse input, ‘IDFT’ is the inverse discrete Fourier transform,  $\mathbf{S}_{\alpha 1}$  is a vector of the measured values of the forward voltage gain (where  $\alpha$  can be either 2, 3 or 4) corresponding to the vector of frequencies,  $\mathbf{f}$ , at which  $\mathbf{S}_{\alpha 1}$  was sampled (and  $\odot$  denotes element-wise multiplication),  $\eta_{tx}$  is the transmit antenna efficiency and  $\eta_{rx}$  is the receive antenna efficiency. The antenna efficiencies were previously measured by S. Bhatti [20]. This method of estimating the impulse response from data measured in the frequency domain can be thought of as using a rectangular window. This leads to a truncation error, however as the maximum measured time constant was 26.6 ns, and the truncation occurs after 200 ns (i.e., for our frequency sweep), we consider this error to be acceptably small.

#### B. Investigating the effect of external objects on the cavity time constant

This measurement took place in the vehicle-like cavity within the SMART anechoic chamber. An Agilent Technologies N5242A two-port VNA was used, with each port connected to Schwarzbeck 9113 antennas, located at (930, 750, 585) mm and (330, 210, 500) mm for ports 1 and 2 respectively, both polarised to align with the  $x$ -axis. A frequency sweep was performed from 1 to 3 GHz, at a resolution of 5 MHz. Two locations were used for the external objects, firstly the location close to the window on the plane  $x = 0$  mm, referred to as A, and secondly the location close to the window on the plane  $y = 1050$  mm, referred to as B, these locations are shown in Figure 2. Four different scenarios were measured:

- 1) SMART chamber unoccupied;
- 2) A person standing approximately 100 mm from the box at location A;
- 3) A standing person holding a large metal plate parallel to the box side at location A, approximately 300 mm from the box;
- 4) A standing person holding a large metal plate parallel to the box side at location B, approximately 300 mm from the box.

Five frequency sweeps were performed for each scenario, and we have processed the data for each – demonstrating similar results in each case. The method detailed previously in Section II-A was used to find the impulse response.

#### C. Investigating the variation of time constant of an actual vehicle, with differing numbers of occupants

Frequency sweeps were performed in actual road vehicles, such that under a variety of loading scenarios the time

constants of the vehicle could be found (i.e., via a IDFT), and compared to those of the vehicle-like cavity. The frequency sweep was again performed from 1 to 3 GHz, with a step size 5 MHz, and the same process as that described in Section II-A was undertaken to find the impulse response from the frequency sweep.

In the road car a Rohde & Schwarz ZVRE two-port VNA was used with each port connected to Schwarzbeck 9113 antennas. The antenna connected to port 1 remained in the boot throughout (as shown in Figure 3, and the antenna connected to port 2 was positioned and orientated arbitrarily in the passenger compartment. The vehicle was measured with each of 0 to 5 passengers occupying it and for each of these loading scenarios 6 different antenna configurations were investigated.

In the panel van a Rohde & Schwarz ZVB8 two-port VNA was used with each port connected to Schwarzbeck 9113 antennas. The antenna connected to port 2 remained in the same location in the footwell close to the passenger side door throughout and the antenna connected to port 1 was positioned and orientated arbitrarily in the passenger compartment. The vehicle was measured with each of 0 to 3 passengers occupying it, and again for each of these loading scenarios 6 different antenna configurations were investigated. A further experiment was undertaken where 6 measurements were taken with the two antennas were located and orientated at random in the rear compartment of the van.

#### D. Simulation to investigate the angular spread

To investigate the angular spread, a simple ray tracing propagation simulation was run for the vehicle-like cavity. This consisted of geometrically tracing a number of rays originating at a transmitter, and considering them to be received if they passed within a cross-sectional area equal to the effective aperture of a perfect isotropic receiver (i.e., in the form of a circle centred on the receiver). The number of reflections was counted, and the power adjusted (using a reflection co-efficient of 0.97) to make the simulation time constant consistent with that of the measurements, the total transmitted power was set equal to 1. While 0.97 may seem low, considering the corroded surfaces, slightly more complex cavity geometry (for example lips around the apertures) and presence of the stirrer, this is not unreasonable. A stirrer was included in the simulation, with a much simplified geometry (i.e., it consisted of a single plane at a slant, in the same location and with approximately the same dimensions as the actual stirrer).

For each ray, the arriving power was recorded along with the angle of arrival. Three simulations were run; and for each the transmitter was located at the same position as port 1 in the measurements detailed in Section II-A, and likewise the receivers were located at the same positions as ports 2, 3 and 4. These three simulations led to similar results, therefore only results from the simulation with the receiver at the same location as port 2 is presented here.

#### E. Spatial E-field variation data

A simulation of the E-field in the vehicle-like cavity was undertaken using CST Microwave Studio. In the simulation, some typical vehicle furniture was also included, this was the same as that previously used in the SEFERE project [21]. For the simulation, the transmit antenna is mounted horizontally near the window, and the E-field is recorded as six axis values (i.e., real and imaginary parts for each of three spatial dimensions) for horizontal cuts each 100 mm, and within each plane at a resolution of 58.6 mm.

### III. INVESTIGATING THE VALIDITY OF REVERBERATION CHAMBER PROPERTIES IN VEHICLE CAVITIES

The measurements are used to investigate the five properties of reverberation chambers introduced in Section I.

#### A. Investigating the power delay profile of in-vehicle channels

Reverberation chamber property 1), from Section I means that the Power Delay Profile (PDP) for a wireless link in a reverberation chamber decays exponentially (where we define a link as the communication channel between two antennas at known locations, the term link is used to avoid ambiguity with ‘channel’ which is used for different communication frequencies for any given link):

$$\bar{P} = ke^{-\frac{t}{\tau}}, \quad (2)$$

where  $\bar{P}$  is the PDP and  $k$  is a constant.

Previous work has shown that it is indeed the case that in general links in electromagnetic cavities have exponentially decaying PDPs [7]. It is not, however, necessarily the case that the time constant of the exponential decay is the same for each link. We therefore estimate the time constant for each link by fitting a minimum mean squared error (MMSE) straight line fit to the exponential decay (plotted in semi-logarithmic form), examples of which are shown in Figures 6 and 7.

Table I shows the time constant estimates for all the links in the vehicle-like cavity and the actual vehicles. For the measurements in the vehicle like cavity,  $\tau_1 - \tau_6$  refer to  $\tau_{xz}$ ,  $\tau_{xx}$ ,  $\tau_{xy}$ ,  $\tau_{zz}$ ,  $\tau_{zx}$  and  $\tau_{zy}$  respectively, and ‘loading’ refers to the number of units of RAM. For the measurements in the actual vehicles,  $\tau_1 - \tau_6$  refer to various random antenna locations (and orientations), and ‘loading’ refers to the number of human occupants.  $\bar{\tau}$  refers to the average of the six time constants, for each environment and loading scenario. It can be seen that for all vehicles and loading configurations, it is indeed the case that the time constant is approximately equal for all links.

#### B. Investigating whether vehicle cavities can be modelled as isolated environments

To investigate whether the vehicle-like cavity is an isolated environment, we evaluated the time constant obtained from

TABLE I  
TIME CONSTANT AND Q-FACTOR ESTIMATION FOR A VEHICLE-LIKE CAVITY, AND ACTUAL VEHICLES.

Location	Loading	$\tau_1$ / ns	$\tau_2$ / ns	$\tau_3$ / ns	$\tau_4$ / ns	$\tau_5$ / ns	$\tau_6$ / ns	$\bar{\tau}$ / ns	2.4 GHz	
									$Q_\tau$	$Q_{PA}$
Vehicle-like cavity	0	22.9	22.8	24.0	26.6	24.5	24.0	24.1	363	85.2
Vehicle-like cavity	4	17.0	16.2	17.6	17.6	17.7	18.6	17.4	262	64.0
Vehicle-like cavity	8	14.3	12.9	13.6	13.6	14.5	15.7	14.1	213	43.6
Vehicle-like cavity	12	13.4	12.1	12.5	13.8	12.8	11.9	12.7	192	38.0
Road car	0	12.0	15.2	15.9	13.0	11.6	14.9	13.8	208	131
Road car	1	10.9	12.2	13.3	11.8	12.6	11.5	12.1	182	115
Road car	2	10.3	11.0	12.8	12.6	10.3	10.7	11.3	170	199
Road car	3	12.8	10.1	11.3	10.6	12.4	12.2	11.6	175	93.9
Road car	4	9.83	11.4	10.5	13.1	10.8	9.81	10.9	164	141
Road car	5	10.1	11.4	10.8	9.53	10.4	12.6	10.8	163	54.9
Van (front)	0	12.1	13.4	15.3	13.5	12.6	13.8	13.4	203	74.9
Van (front)	1	10.2	9.88	11.0	10.1	9.71	9.87	10.1	153	42.0
Van (front)	2	7.46	8.08	9.80	10.8	7.63	7.78	8.58	129	38.6
Van (front)	3	8.31	8.89	9.07	9.32	10.2	6.43	8.71	131	31.0
Van (rear)	n/a	19.0	16.6	18.7	23.4	18.1	20.0	19.3	291	69.3

'Loading' in the vehicle-like cavity refers to the number of units of RAM, whereas in the actual vehicles it refers to the number of occupants.

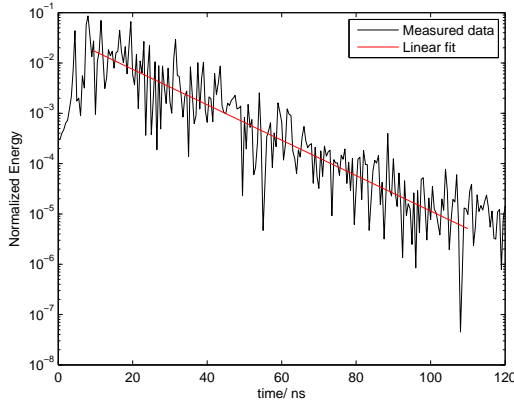


Fig. 6. Example of exponential decay, vehicle-like cavity loaded with 12 units of RAM.

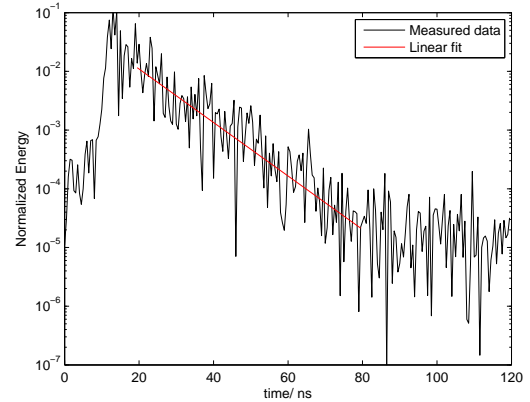


Fig. 7. Example of exponential decay, road car loaded with 5 occupants.

the measurements detailed in Section II-B, where the external environment is varied. Once again we used an MMSE estimator (in semi-logarithmic axes) to find an estimate of  $\tau$ . Our results, shown in Table II, provide evidence that the time constant does not vary significantly as a result of changes in the external environment and thus the vehicle-like cavity can indeed be treated as an isolated environment. In general, the noise floor may have to be raised, to account for propagation into the cavity of radiation from external sources.

### C. Investigating the E-field uniformity in vehicle cavities

An important metric for reverberation chambers is the Quality (Q) factor, which can be related to the cavity time constant:

$$Q_\tau = 2\pi f\tau, \quad (3)$$

TABLE II  
TIME CONSTANT ESTIMATION.

Scenario	$\tau$ / ns	$Q_\tau$ 2.4 GHz
Empty Chamber	23.3	352
Man at A	23.1	349
Metal at A	22.8	343
Metal at B	23.0	348

where  $f$  is the frequency.

An alternative method to find the Q-factor is using a Power Average (PA) method:

$$Q_{PA} = \frac{16\pi^2 V}{\eta_{tx}\eta_{rx}\lambda^3} \left\langle \frac{P_r}{P_t} \right\rangle, \quad (4)$$

where  $\eta_{tx}$  and  $\eta_{rx}$  are the efficiencies of the transmitting and receiving antennas respectively and  $V$  is the volume of the

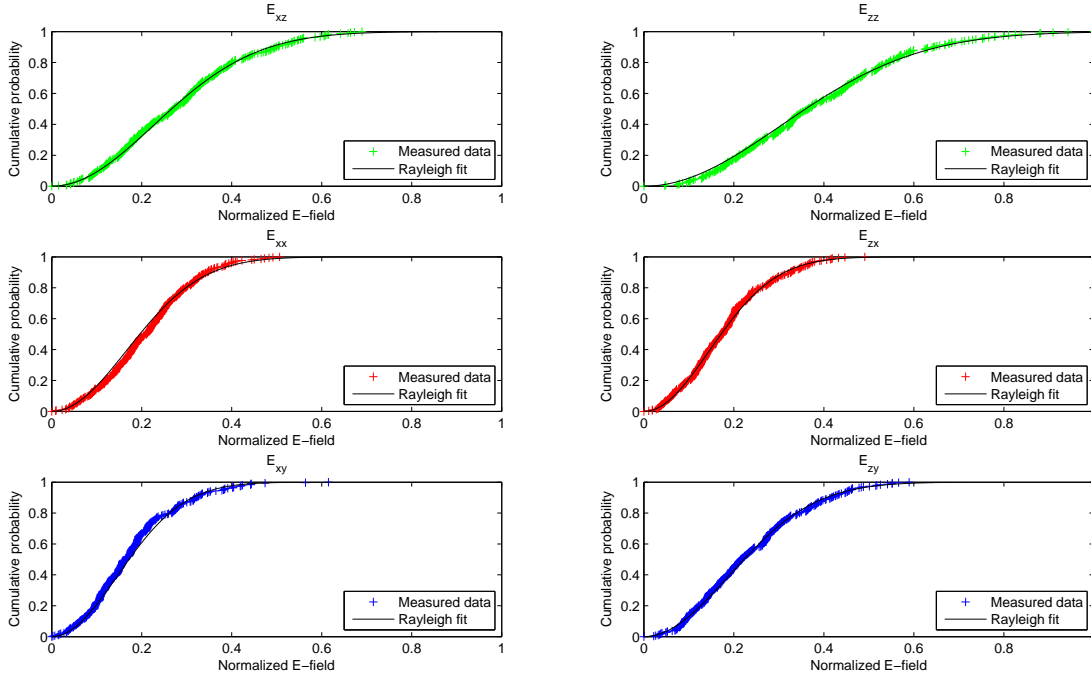


Fig. 8. Example of E-Field distribution in the vehicle like cavity at 2.4 GHz (i.e., above the theoretical LUF), with the cavity not loaded.

cavity. The derivation of (4) in [ [17] Section 7.6], assumes only that the energy density is constant throughout the cavity, and therefore  $Q_\tau = Q_{PA}$  is a necessary and sufficient condition for the E-field to be homogeneous.

To find  $Q_{PA}$  for the vehicle-like cavity and vehicles, the average  $\langle P_\tau/P_t \rangle$  was taken over all links, and for all frequency samples over a bandwidth of 100 MHz bandwidth (i.e., the frequency stirring introduced in Section II-A). For the vehicle like cavity, the independent stirrer positions were also included in the average. The results are shown in Table I, and clearly  $Q_\tau \neq Q_{PA}$ , therefore the E-field is not homogeneous. Also note that the time constant and Q-factor decrease with loading, which is consistent with previous work [22].

An isotropic field means that over an arbitrary set of frequencies or stirrer positions, the distribution of the received signal (which is proportional to one Cartesian component of the E-field at the location of the receive antenna) will correspond to a circularly symmetric Gaussian random variable (i.e., its magnitude will be Rayleigh distributed). A plot for the measured field distributions at 2.4 GHz (i.e., over all independent stirrer positions and 100 MHz bandwidth) for each of the 6 channels is shown in Figure 8. The E-field was found by noting that  $S_{\alpha 1} \propto E\text{-field}_{\alpha 1}$ , and the E-field was normalised by setting the greatest sampled value equal to 1.

It can be seen that for each plot, it appears that the Rayleigh distribution is a good fit, and for each of the three pairs where the antenna locations remain the same, but one

antenna is rotated to be orthogonal (i.e., the three horizontally adjacent pairs) the distributions are similar, as would be the case an isotropic field. It can therefore be concluded that there is evidence that the field is slightly degraded from ideal isotropic conditions, but there is still strong correlation between orthogonal field distributions at any point.

It is important to consider the lowest frequency at which a field distribution which is close to isotropic can be obtained, this is termed the Lowest Usable Frequency (LUF). There are two conditions required for an isotropic field:

- 1)  $f \gg 1/\tau$ , this is required for a uniform distribution on the phase of the arriving rays.
- 2) There must be 60 modes present in the cavity (this is a good general rule, although there is some evidence that isotropic fields can be obtained below this frequency [23]). Strictly speaking this is only valid if the stirrer is very efficient, or there are two independent stirrers, which isn't the case in the vehicle-like cavity (and it is not clear to what extent the frequency stirring mitigates this), therefore the 60 mode rule can only be used as a guideline in this case.

For a rectangular cavity, 60 modes are present at a frequency approximately 3 times the lowest resonant frequency. The lowest resonant frequency can be found from [24], and for our cavity this is 342 MHz, therefore the 60 mode rule should apply at frequencies above 1.03 GHz. The lowest value of  $\tau$  is 12.7 ns, when the cavity is loaded with 12 units of RAM, therefore  $1/\tau = 78.7 \times 10^6$ , and so it is reasonable to say  $f \gg 1/\tau$ .

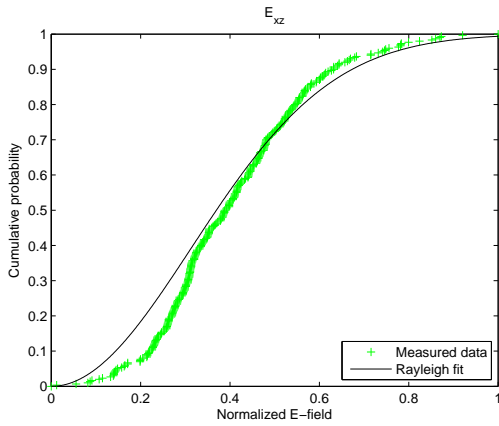


Fig. 9. Example of E-Field distribution in the vehicle like cavity at 600 MHz (i.e., below the theoretical LUF), with the cavity loaded with 12 units of RAM.

The effect of loading not only has an effect on the time constant, it also potentially effects the number of modes, with greater loading leading to fewer modes [25] and therefore a greater LUF. It has also, however, been reported that the opposite effect may happen for example, Arnaut shows that the LUF is proportional to the third root of the Q-factor (and hence time constant) [26].

To determine whether the field distribution is isotropic at a given frequency, we take a subjective approach, by observing the appearance of the fit of the Rayleigh distribution and the similarity of the orthogonally polarised channel pairs for given antenna locations. It can also be shown that for a Rayleigh distribution the ratio of the mean to the standard deviation is 1.91, and this can be compared to the same ratio for the measured data to further investigate the goodness of fit of the Rayleigh distribution. Our results show that a field distribution which is close to isotropic can be obtained at frequencies greater or equal to 1.7 GHz and 2.7 GHz for the cavity loaded with 0 and 4 units of RAM respectively, for 8 and 12 units of RAM an isotropic field is not obtained even at the maximum frequency of 2.9 GHz. Therefore it appears that the LUF to obtain an isotropic field is sensitive to the amount of loading. Figure 9 shows an example of the E-field distribution at 600 MHz and it can be seen that the Rayleigh distribution is not a good fit. It should be noted that while we take a subjective approach, for any given application an objective criteria for an isotropic field could be defined and used to find the LUF.

It is important to know whether the field is isotropic or not to deploy effective communication systems. For example it can be shown (as to be discussed in more detail in Section IV) that if the field is isotropic, and homogeneous over a small area, then the spatial correlation is well defined, which is useful for Multiple-Input-Multiple-Output (MIMO) systems [17]. Furthermore, information theoretic analysis on the channel capacity typically assumes that the received signal has the form of a zero-mean circularly symmetric complex Gaussian distribution [27], and this will be the case if the field

is isotropic. Should it be required to use frequencies below the LUF, a useful body of literature concerning probability distributions for E-fields in non ideal conditions is available, for example [28].

#### IV. USING REVERBERATION CHAMBER PROPERTIES TO IMPROVE COMMUNICATION SYSTEMS IN VEHICLES

To establish exactly how the reverberation chamber analysis can lead to improved estimates of wireless communication parameters, we define a cavity classification system:

- Type I: Properties 1)-5) (in Section I) all apply, and thus full reverberation chamber analysis can be applied.
- Type II:  $\tau$  is equal for all possible links in the cavity (i.e., regardless of the locations of antennas and any moveable internal objects). The cavity can be treated as an isolated environment. Type II is further divided:
  - II A: At a point, the E-field distribution is isotropic (at a sufficiently high frequency).
  - II B: At a point, the E-field distribution is not necessarily isotropic.
- Type III:  $\bar{P} = ke^{-\frac{t}{\tau}}$  applies to all possible links in the cavity, but the value  $\tau$  varies from link to link. The environment is not necessarily isolated.

Our measurements presented in Table I show that the Type II channel model is appropriate for vehicle cavities. The subdivision of Type II cavities is useful for establishing the spatial and angular distributions for MIMO applications.

##### A. In-vehicle channel root mean square delay spread

The channel RMS delay spread is an important parameter for effective wireless communication system deployment. Theoretically, in Type II cavities the RMS delay spread should be the same for each link in the cavity (as the PDP is the same for each link). It can be shown that the theoretical RMS delay spread ( $\sigma_{\text{rms}}$ ) is equal to the cavity time constant. Comparing the actual value of  $\sigma_{\text{rms}}$  from the measurements to the cavity time constant for each environment and loading configuration, as detailed in Table III, it can be seen that it is indeed the case that the RMS delay is approximately equal to the cavity time constant.

This means that the delay spread, and hence also coherence bandwidth, is common for all links in a Type II cavity (which has been shown to be a good model for many vehicle cavities). This property can be exploited by wireless communication system designers, for example if the cavity time constant is known then when a link is first turned on, there will immediately be information available regarding its delay spread and coherence bandwidth prior to any direct channel estimation. Furthermore, it should be possible to aggregate data from many different links to improve the estimate of the cavity time constant.

From the RMS delay spread, the channel coherence time can be found. Using the same definition of coherence bandwidth

TABLE III  
RMS DELAY SPREAD VALUES.

Environment	Loading	$\bar{\tau}$ / ns	$\sigma_{\text{rms 1}}$ / ns	$\sigma_{\text{rms 2}}$ / ns	$\sigma_{\text{rms 3}}$ / ns	$\sigma_{\text{rms 4}}$ / ns	$\sigma_{\text{rms 5}}$ / ns	$\sigma_{\text{rms 6}}$ / ns
Vehicle-like cavity	0	24.1	23.1	23.4	23.5	21.1	24.3	23.7
Vehicle-like cavity	4	17.4	18.5	16.1	18.4	14.3	18.1	16.7
Vehicle-like cavity	8	14.1	13.7	14.0	15.7	11.0	15.3	14.4
Vehicle-like cavity	12	12.7	12.8	11.9	12.0	9.10	12.0	12.0
Road car	0	13.8	13.3	13.3	13.5	12.2	11.4	14.0
Road car	1	12.1	11.9	12.1	12.5	9.93	12.7	11.4
Road car	2	11.3	10.4	10.6	12.7	12.0	8.96	10.6
Road car	3	11.6	11.3	10.0	10.7	10.6	11.4	10.9
Road car	4	10.9	9.56	11.7	10.6	10.9	10.4	10.7
Road car	5	10.8	10.2	10.8	10.4	9.58	10.3	13.1
Van (front)	0	13.4	10.0	12.0	12.9	9.80	10.7	12.4
Van (front)	1	10.1	8.55	10.6	11.5	9.47	8.49	10.2
Van (front)	2	8.58	6.56	7.63	8.20	10.4	8.09	7.06
Van (front)	3	8.71	6.75	8.39	8.46	9.08	9.35	5.24
Van (rear)	n/a	19.3	19.4	17.6	18.2	19.9	18.6	19.0

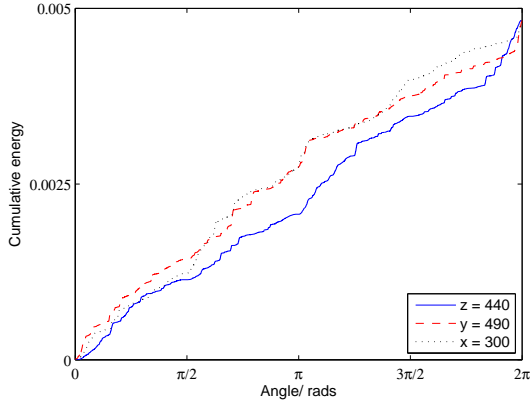


Fig. 10. Angular spread at 2.4 GHz for three orthogonal planes (i.e.,  $z = 440$ ,  $y = 490$ ,  $x = 300$ )

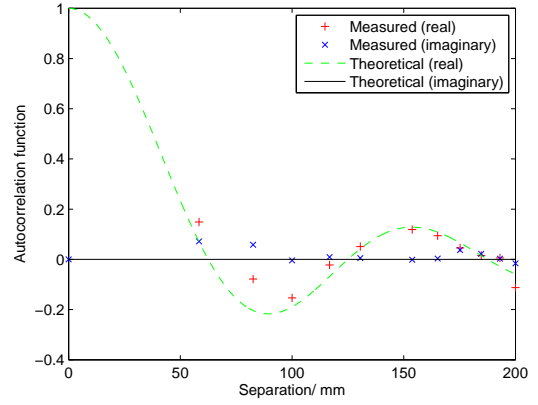


Fig. 11. Spatial correlation at 2.4 GHz.

( $B_c$ ) as Liu *et al* [19], that the autocorrelation co-efficient is greater than 0.5, then  $B_c = 1/(5\sigma_{\text{rms}})$ . For the environment and loading configurations measured the time constant was found to be between 8.58 and 24.1 ns, leading to coherence bandwidths in the range 8.30 to 23.3 MHz, which is consistent with previous work [19].

### B. In-vehicle channel angular spread

The angular spread is important for determining whether beamforming can lead to improvements in wireless systems deployed in vehicles. Given the unoccupied vehicle-like cavity has been shown to have an isotropic field distribution at 2.4 GHz, it is expected that the angular spread will be uniform. This is confirmed by the ray tracing propagation simulation (i.e., as detailed in Section II-D, with the results shown in Figure 10 for the angular spread in three orthogonal planes.

There is, however, some evidence that in actual vehicles, certain channels may not have a uniform angular spread [29]. In such cases, beamforming may be used to enhance performance.

### C. In-vehicle channel coherence distance

For the vehicle-like cavity, it has been shown that the E-field distribution is isotropic at 2.4 GHz. This is supported by a ray-tracing simulation, which provides evidence that the angular spread is approximately uniform. Furthermore, by evaluating the total received power at various locations in close proximity using the ray-tracing simulation, it appears that the total received power varies continuously in space. Therefore, over sufficiently short distances, the E-field can be thought of as being locally homogeneous. In such cases, the spatial correlation is well defined.

Figure 11 compares the measured spatial correlation to the theoretical spatial correlation at 2.4 GHz (i.e., from [17] Equation (7.48)), where it can be seen that there is

some evidence that the theoretical model may apply. Note that, for the theoretical results, the imaginary component is always equal to zero, therefore this line appears as the  $x$ -axis. This is important for the design of MIMO antenna arrays, where the spatial correlation leads directly to the choice of antenna element spacing.

In vehicle and vehicle-like cavities, the properties of spatial correlation and angular spread can be thought of as complementary. In Type IIA cavities, where the field distribution is isotropic, the spatial correlation is well defined and thus MIMO can be used to improve performance. In Type IIB cavities, the spatial correlation is not necessarily well defined, however beam-forming can be used to exploit the non-uniformity of the angular spread.

## V. CONCLUSIONS

This paper details a thorough assessment of the analogy between vehicle and vehicle-like cavities, with reverberation chambers. Specifically, the cavity time constant, electromagnetic isolation and E-field uniformity of typical vehicle cavities are investigated.

It is found that, under all operating scenarios, the time-constant is approximately the same for all possible links in typical vehicle cavities, and that they can be treated as isolated electromagnetic environments. For the E-field distribution to be uniform, it must be homogeneous and isotropic, which is not generally the case in vehicle cavities. It is, however, the case that in some situations the E-field is isotropic.

These properties can potentially be used to improve the performance of wireless systems deployed in vehicles. For example, that the time constant is the same for all possible links in a given cavity, leads to the property that the RMS delay spread is also the same for all links. This is potentially very useful, as it allows the wireless system to have some information regarding the channel state before a link is even active. For example, the RMS delay spread can be used to find the coherence bandwidth, and thus frequency diversity can be used in an intelligent way immediately when a link is turned on. Likewise, if for a given cavity, the E-field distribution is isotropic, then it has been shown that the spatial correlation is well defined, and thus deployment of MIMO antenna arrays should prove effective. If the E-field distribution is not isotropic, then it follows that the angular spread is not uniform, and thus beamforming can be used.

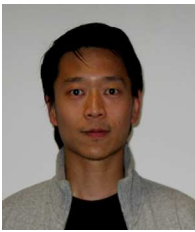
## REFERENCES

- [1] J. Dawson, D. Hope, M. Panitz, and C. Christopoulos, "Wireless networks in vehicles," in *Electromagnetic Propagation in Structures and Buildings, 2008 IET Seminar on*, dec. 2008, pp. 1–6.
- [2] G. Leen and D. Heffernan, "Vehicles without wires," *Computing Control Engineering Journal*, vol. 12, no. 5, pp. 205–211, Oct 2001.
- [3] J. Andersen, K. L. Chee, M. Jacob, G. Pedersen, and T. Kurner, "Reverberation and absorption in an aircraft cabin with the impact of passengers," *IEEE Transactions on Antennas and Propagation*, vol. 60, no. 5, pp. 2472–2480, May 2012.
- [4] M. Heddebaut, V. Deniau, and K. Adouane, "In-vehicle wlan radio-frequency communication characterization," *IEEE Transactions on Intelligent Transportation Systems*, vol. 5, no. 2, pp. 114–121, June 2004.
- [5] A. Ruddle, "Validation of simple estimates for average field strengths in complex cavities against detailed results obtained from a 3d numerical model of a car," *Science, Measurement Technology, IET*, vol. 2, no. 6, pp. 455–466, November 2008.
- [6] H. Weng, D. Beetmer, T. Hubing, X. Dong, R. Wiese, and J. McCallum, "Investigation of cavity resonances in an automobile," in *International Symposium on Electromagnetic Compatibility, 2004.*, vol. 3, 2004, pp. 766–770 vol.3.
- [7] S. Herbert, T. H. Loh, and I. Wassell, "An impulse response model and Q-factor estimation for vehicle cavities," *IEEE Transactions on Vehicular Technology*, vol. 62, no. 9, pp. 4240–4250, 2013.
- [8] S. Herbert, I. Wassell, T. Loh, and J. Rigelsford, "Characterizing the spectral properties and time variation of the in-vehicle wireless communication channel," *Communications, IEEE Transactions on*, vol. 62, no. 7, pp. 2390–2399, July 2014.
- [9] [Online]. Available: <https://www.cst.com/Products/CSTMWS>
- [10] [Online]. Available: <http://www.sefere.org/>
- [11] H. Zhang, L. Low, J. Rigelsford, and R. Langley, "Field distributions within a rectangular cavity with vehicle-like features," *Science, Measurement Technology, IET*, vol. 2, no. 6, pp. 474–484, November 2008.
- [12] A. Ruddle, "Impact of internal dielectric components for vehicle models," 2010.
- [13] L. Low, H. Zhang, J. Rigelsford, and R. Langley, "Computed field distributions within a passenger vehicle at 2.4 ghz," in *Antennas Propagation Conference, 2009. LAPC 2009. Loughborough*, Nov 2009, pp. 221–224.
- [14] —, "Measured and computed in-vehicle field distributions," in *Antennas and Propagation (EuCAP), 2010 Proceedings of the Fourth European Conference on*, April 2010, pp. 1–3.
- [15] [Online]. Available: <http://www.schwarzbeck.de/Datenblatt/k9113.pdf>
- [16] [Online]. Available: [http://webstore.iec.ch/webstore/webstore.nsf/ArtNum\\_PK/44777?OpenDocument](http://webstore.iec.ch/webstore/webstore.nsf/ArtNum_PK/44777?OpenDocument)
- [17] D. Hill, *Electromagnetic Fields in Cavities (Deterministic and Statistical Theories)*. IEEE Press, Piscataway, NJ, 2009.
- [18] T. A. Loughry, "Frequency stirring: an alternative approach to mechanical mode-stirring for the conduct of electromagnetic susceptibility testing," in *Phillips Laboratory, Kirtland Air Force Base, NM Technical Report 91-1036*, 1991.
- [19] R. Liu, S. Herbert, T.-H. Loh, and I. Wassell, "A study on frequency diversity for intra-vehicular wireless sensor networks (wsns)," in *Vehicular Technology Conference (VTC Fall), 2011 IEEE*, 2011, pp. 1–5.
- [20] S. Bhatti, "Cross-correlate methods for antenna efficiency measurement in acechoic and reverberation chamber," Master's thesis, University of Surrey, 2010.
- [21] H. Zhang, L. Low, J. Rigelsford, and R. Langley, "Effects of vehicle furnishings on performance of aperture mounted multi-band conformal automotive antenna," in *Antennas and Propagation, 2009. EuCAP 2009. 3rd European Conference on*, March 2009, pp. 2694–2697.
- [22] E. Genender, C. Holloway, K. Remley, J. Ladbury, G. Koepke, and H. Garbe, "Use of reverberation chamber to simulate the power delay profile of a wireless environment," in *Electromagnetic Compatibility - EMC Europe, 2008 International Symposium on*, Sept 2008, pp. 1–6.
- [23] M. Hatfield, M. Slocum, E. Godfrey, and G. Freyer, "Investigations to extend the lower frequency limit of reverberation chambers," in *IEEE International Symposium on Electromagnetic Compatibility.*, vol. 1, August 1998, pp. 20–23 vol.1.
- [24] J. Dawson and L. Arnaut, "Reverberation (mode-stirred) chambers for electromagnetic compatibility." [Online]. Available: [http://www.compliance-club.com/archive/old\\_archive/030530.htm](http://www.compliance-club.com/archive/old_archive/030530.htm)
- [25] O. Lunden and M. Backstrom, "Absorber loading study in foI 36.7 m<sup>3</sup> mode stirred reverberation chamber for pulsed power measurements," in *IEEE International Symposium on Electromagnetic Compatibility.*, August 2008, pp. 1–5.
- [26] L. Arnaut, "Compound exponential distributions for undermoded reverberation chambers," *Electromagnetic Compatibility, IEEE Transactions on*, vol. 44, no. 3, pp. 442–457, Aug 2002.
- [27] G. Durisi, U. Schuster, H. Bolcskei, and S. Shamai, "Noncoherent capacity of underspread fading channels," *Information Theory, IEEE Transactions on*, vol. 56, no. 1, pp. 367–395, Jan 2010.
- [28] R. Serra and F. Canavero, "Bivariate statistical approach for "good-but-imperfect" electromagnetic reverberation," *Electromagnetic Compatibility, IEEE Transactions on*, vol. 53, no. 3, pp. 554–561, Aug 2011.
- [29] H. Sawada, T. Tomatsu, G. Ozaki, H. Nakase, S. Kato, K. Sato, and H. Harada, "A sixty GHz intra-car multi-media communications system,"

in *Vehicular Technology Conference, 2009. VTC Spring 2009. IEEE 69th*, 2009, pp. 1–5.



**Steven Herbert** (S12) received the B.A. degree [subsequently promoted to M.A. (Cantab) in 2013] from the University of Cambridge, Cambridge, U.K., in 2010 and the M.Eng. degree. He is currently working towards the Ph.D. degree with the University of Cambridge. He is currently with the Digital Technologies Group, Computer Laboratory, University of Cambridge, and the Electromagnetic Technologies Group, National Physical Laboratory, Middlesex, U.K.



**Tian Hong Loh** (S'03-M'05) was born in Johor, Malaysia. He received the B.Eng. degree (first class) from Nottingham Trent University, Nottingham, U.K., and the Ph.D. degree from the University of Warwick, Coventry, U.K., in 1999 and 2005, respectively, both in electrical and electronic engineering. He joined the National Physical Laboratory, Teddington, U.K., in 2005 as a Higher Research Scientist and since 2009 he has been a Senior Research Scientist, involved in work on fundamental research and develop measurement technologies in

support of the electronics and communication industry. Since 2011, he has been appointed as RF and Microwave technical theme leader, involved in physical programme formulation and strategy development. His current research interests include metamaterials, computational electromagnetics, small antenna, smart antennas, and wireless sensor networks.



**Ian Wassell** received his B.Sc. and B.Eng. degrees from the University of Loughborough in 1983, and his Ph.D. degree from the University of Southampton in 1990. He is a Senior Lecturer at the University of Cambridge Computer Laboratory and has in excess of 15 years experience in the simulation and design of radio communication systems gained via a number of positions in industry and higher education. He has published more than 170 papers concerning wireless communication systems and his current research interests include: fixed wireless access, sensor networks, cooperative networks, propagation modelling, compressive sensing and cognitive radio. He is a member of the IET and a Chartered Engineer.

sensor networks, cooperative networks, propagation modelling, compressive sensing and cognitive radio. He is a member of the IET and a Chartered Engineer.



**Jonathan Rigelsford** (SM'13) received the MEng and PhD degrees in Electronic Engineering from the University of Hull, Hull, UK in 1997 and 2001 respectively. From 2000 to 2002, he worked as Senior Design Engineer at Jaybeam Limited, designing antennas for cellular base stations. Since late 2002, he has been a Senior Experimental Officer for the Communications Group within the Department of Electronic and Electrical Engineering, University of Sheffield, Sheffield, UK. He is also a Senior Research Fellow at the same institution. Dr Rigelsford

has been an active member of the Antenna Interface Standards Group (AISG) from 2002 to 2010 being elected to the board of directors during that time. More recently, he has become Secretary to the Wireless Friendly Building Forum, an industrial/academic initiative to promote understanding of radio propagation within the built environments.